

# On the symmetry of efficiency-versus-carrier-concentration curves in GaInN/GaN light-emitting diodes and relation to droop-causing mechanisms

Qi Dai,<sup>1</sup> Qifeng Shan,<sup>1</sup> Jaehee Cho,<sup>1</sup> E. Fred Schubert,<sup>1,a)</sup> Mary H. Crawford,<sup>2</sup> Daniel D. Koleske,<sup>2</sup> Min-Ho Kim,<sup>3</sup> and Yongjo Park<sup>3</sup>

<sup>1</sup>Department of Physics, Applied Physics and Astronomy and Department of Electrical, Computer, and Systems Engineering, Rensselaer Polytechnic Institute, Troy, New York 12180, USA

<sup>2</sup>Sandia National Laboratories, Albuquerque, New Mexico 87185, USA

<sup>3</sup>R&D Institute, Samsung LED, Suwon 443-743, Republic of Korea

(Received 2 December 2010; accepted 3 January 2011; published online 20 January 2011)

The internal quantum efficiency (IQE)-versus-carrier-concentration ( $n$ ) curves of GaN-based light-emitting diodes have been frequently described by the  $ABC$  model:  $\text{IQE} = Bn^2 / (An + Bn^2 + Cn^3)$ . We show that this model predicts IQE-versus- $n$  curves that have even symmetry. Phase-space filling makes the  $B$  and  $C$  coefficients concentration-dependent. We also show that IQE-versus- $n$  curves that take into account phase-space filling possess even symmetry. In contrast, experimental IQE-versus- $n$  curves exhibit asymmetry. The asymmetry requires a fourth-power or higher-power contribution to the recombination rate and provides insight into the mathematical form of the droop-causing mechanisms. © 2011 American Institute of Physics. [doi:10.1063/1.3544584]

The “efficiency droop,” which is the gradual decrease of efficiency as the injection-current density surpasses a low value that is typically between 0.1 and 10 A/cm<sup>2</sup>, is a unique characteristic of GaN-based light-emitting diodes (LEDs).<sup>1–9</sup> The internal quantum efficiency (IQE) of GaN-based LEDs has been frequently described by the  $ABC$  model,  $\text{IQE} = Bn^2 / (An + Bn^2 + Cn^3)$ , where  $A$ ,  $B$ , and  $C$  represent the Shockley–Read–Hall (SRH) and radiative and Auger coefficients, respectively,<sup>5–7</sup> and  $n$  represents carrier concentration. The  $B$  and  $C$  coefficients become concentration-dependent when taking into account phase-space filling.<sup>7,8</sup> We show that based on the  $ABC$  model, the IQE-versus- $n$  curve (without and with phase-space filling) has a striking feature, namely, even symmetry. In contrast, for a wide variety of samples, experimental IQE-versus- $n$  curves exhibit asymmetry. The asymmetry requires a fourth-power or higher-power contribution to the recombination rate and provides insight into the mathematical form of the droop-causing mechanisms.

Two types of GaN-based LEDs are grown on  $c$ -plane sapphire substrates by metal-organic vapor-phase epitaxy. Both of them have a five-period GaInN/GaN multiquantum well (MQW) active region. LED-1 is a commercial LED emitting at approximately 463 nm. The quantum well (QW) thickness is estimated to be 2.5 nm. LED-2 emits at approximately 444 nm. Each QW is 2.3 nm wide separated by 7.5 nm Si-doped GaN barriers. The unencapsulated wafer-level devices are tested under pulsed mode from 10  $\mu$ A to 70 mA ( $200 \times 200 \mu\text{m}^2$  devices) or 100 mA ( $300 \times 300 \mu\text{m}^2$  devices) with 500  $\mu$ s pulse duration and 1% duty cycle. Junction heating is not anticipated to be a factor under the employed pulsed conditions since the thermal time constant of the devices is in the millisecond range.<sup>10</sup> The lack of heating effects is verified by the fact that shorter pulse widths (from 5 to 500  $\mu$ s, 1% duty cycle) do not change results for the applied injection-current range.

According to the  $ABC$  model, light-output power (LOP) is proportional to  $Bn^2$  (or  $\sqrt{\text{LOP}} \propto n$ ), and the IQE can be expressed as follows:

$$\text{IQE} = \frac{Bn^2}{An + Bn^2 + Cn^3} = \frac{B}{A/n + B + Cn}. \quad (1)$$

The peak efficiency is reached when  $d\text{IQE}(n)/dn = 0$ , therefore the carrier concentration at the peak-efficiency point  $n_0 = \sqrt{A/C}$  is obtained. By using Eq. (1), one can show that for any  $n_1 = kn_0$  and  $n_2 = n_0/k$  (where  $k$  is a scaling factor which could be any positive constant), the following condition is satisfied:

$$\text{IQE}(n_1 = kn_0) = \text{IQE}(n_2 = n_0/k) = \frac{B}{B + (k + 1/k)\sqrt{AC}}. \quad (2)$$

This equation shows that the IQE-versus- $n$  curve has even symmetry about the  $n = n_0$  line when the carrier concentration is plotted on a logarithmic abscissa scale. This mathematical finding is illustrated by the solid curve in Fig. 1(a), which shows a theoretical IQE-versus- $n$  curve calculated using  $A = 10^7 \text{ s}^{-1}$ ,  $B = 10^{-10} \text{ cm}^3 \text{ s}^{-1}$ , and  $C = 5 \times 10^{-29} \text{ cm}^6 \text{ s}^{-1}$ .

For experimental IQE-versus- $n$  curves, LED-1 and LED-2 are tested at room temperature. Figure 1(b) shows IQE as a function of  $\sqrt{\text{LOP}}$ , which is proportional to  $n$ . Strong asymmetries about the dashed lines, which go through the peak-efficiency points, can be observed in Fig. 1(b). We find similar asymmetries for LEDs with only 1 QW; therefore, the asymmetry is not caused by the nonuniform distribution of carriers within the MQWs. The technical literature indeed reveals abundant asymmetric IQE-versus- $n$  curves (see, for example, Fig. 2 in Ref. 11). The derivation of the absolute IQE values shown in Fig. 1(b) will be described later in this paper.

The injection current and the carrier concentration are related by (1) low carrier-concentration regime  $I \propto n^{<2}$  (e.g.,  $I \propto n$  for SRH recombination dominating) and (2) high carrier-concentration regime  $I \propto n^{>2}$  (e.g.,  $I \propto n^3$  for Auger re-

a)Electronic mail: efschubert@rpi.edu.

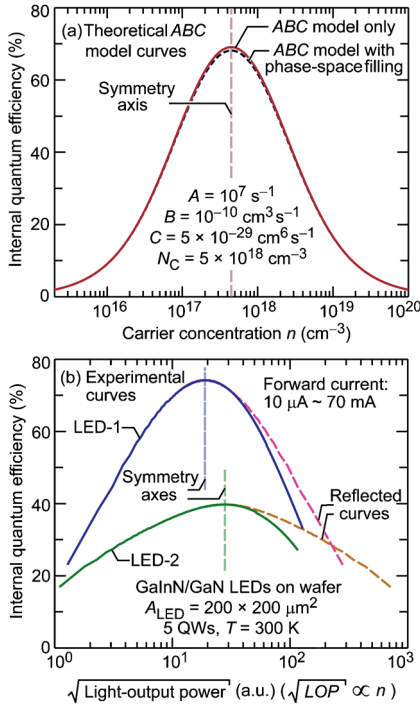


FIG. 1. (Color online) (a) Theoretical IQE-vs- $n$  curves based on the ABC model (without and with phase-space filling) showing even symmetry. (b) Experimental IQE-vs- $\sqrt{\text{LOP}}$  ( $\sqrt{\text{LOP}} \propto n$ ) curves showing asymmetry. The experimental curves are skewed to the left.

combination dominating). Therefore, the evenly symmetric IQE-versus- $n$  curve corresponds to an IQE-versus- $I$  curve which is *skewed to the right*, that is, the IQE-versus- $I$  curve has higher efficiency at high currents than for the symmetric case. This skewed-to-the-right IQE-versus- $I$  property is a necessary condition for the applicability of the ABC model. However, our experiments [see Fig. 2(b), to be discussed later] and the technical literature [see, for example, curves (a) and (c) in Fig. 1 of Ref. 12] reveal that IQE-versus- $I$  curves can be skewed to the left.

Phase-space filling makes the  $B$  and  $C$  coefficients carrier-concentration dependent. The  $B$  and  $C$  coefficients

have been modeled as  $B = B_0/(1 + n/N_C)$  and  $C = C_0/(1 + n/N_C)$ , respectively,<sup>7,8</sup> where  $N_C$  is a constant in the range of  $5 \times 10^{18} - 2 \times 10^{19} \text{ cm}^{-3}$ ,<sup>7</sup> and  $B_0$  and  $C_0$  are radiative and Auger coefficients at low carrier injection, respectively. By inserting the expressions for the  $B$  and  $C$  coefficients into Eq. (1), one obtains

$$\begin{aligned} \text{IQE} &= \frac{\frac{B_0}{1 + n/N_C} n^2}{An + \frac{B_0}{1 + n/N_C} n^2 + \frac{C_0}{1 + n/N_C} n^3} \\ &= \frac{(A/N_C + B_0)}{A/n + (A/N_C + B_0) + C_0 n (A/N_C + B_0)} \cdot \frac{B_0}{n^2}. \end{aligned} \quad (3)$$

Comparing Eq. (3) with Eq. (1), one finds that the IQE-versus- $n$  curve that takes into account phase-space filling possesses even symmetry as well. The dashed curve in Fig. 1(a) shows that the effect of the phase-space filling is relatively small; the dashed curve is obtained by using a relatively small value of  $N_C$ ,  $N_C = 5 \times 10^{18} \text{ cm}^{-3}$ , thereby making the effect of phase-space filling large. Therefore, the asymmetry in the IQE-versus- $n$  curves (e.g., Fig. 2 of Ref. 11) cannot be explained by the ABC model even when taking into account phase-space filling.

Recalling Eq. (1), one can show that besides the SRH and radiative and Auger terms, adding a positive fourth-order (or higher-order) nonradiative term to the recombination-rate equation results in an IQE-versus- $n$  curve skewed to the left, thereby providing a better agreement between experiments and theory. A fourth-order term could be a part of a carrier-loss mechanism, for example, carrier leakage out of the active region.<sup>1,2,9</sup> This carrier-loss mechanism may also have first, second, and third order components, which do not affect the symmetry. In order to further investigate the carrier-loss mechanism that causes asymmetry, we use polynomial fitting to the  $R$ -versus- $n$  data of our LED samples (where  $R$  is the recombination rate). At steady state,  $R$  equals the generation rate  $G$ , and can be obtained from injection current  $I$ , elementary charge  $q$ , and effective active region volume  $V_{\text{active}}$ ,

$$R = G = I/qV_{\text{active}}. \quad (4)$$

The IQE can be expressed as

$$\text{IQE} = Bn^2/R. \quad (5)$$

Then  $n$  is obtained by solving Eqs. (4) and (5) for  $n$ ,

$$n = \sqrt{\frac{\text{IQE} \cdot I}{BqV_{\text{active}}}} = \sqrt{\frac{\text{IQE}_{\text{peak}}}{BqV_{\text{active}}}} \sqrt{\text{IQE}_{\text{normalized}} \cdot I}, \quad (6)$$

where  $\text{IQE}_{\text{peak}}$  is the peak IQE value, and  $\text{IQE}_{\text{normalized}}$  represents normalized IQE (varies between 0 and 1) as a function of current. One can perform a polynomial fit to the  $R$ -versus- $n$  data derived from the experimental  $\text{IQE}_{\text{normalized}}$ -versus- $I$  data using Eqs. (4) and (6). This procedure allows us to expand the recombination rate  $R$  as a polynomial expression of carrier concentration  $n$ , that is  $R = A'n + B'n^2 + C'n^3 + D'n^4 + \dots$ , extract the contribution of each recombination channel ( $A'n$ ,  $B'n^2$ ,  $C'n^3$ , and  $D'n^4$ ), and obtain a theoretical IQE-versus- $I$  curve. We will discuss the meaning of polynomial parameters  $A' \sim D'$  later in this paper.

Figures 2(a) and 2(b) show the experimental IQE-versus- $I$  data and theoretical fits based on the results

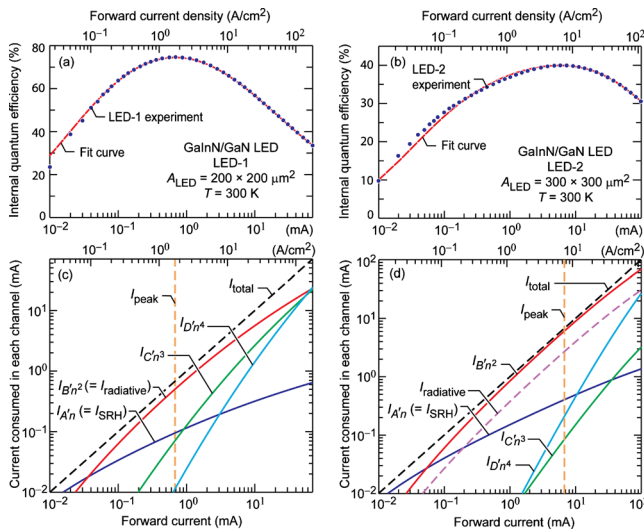


FIG. 2. (Color online) Experimental IQE-vs- $I$  data and theoretical fitting curves for (a) LED-1 and (b) LED-2; current consumed in each recombination channel as a function of forward current for (c) LED-1 and (d) LED-2.

obtained from polynomial fits to the  $R$ -versus- $n$  data (where we have used up-to-fourth-order terms). Figures 2(c) and 2(d) show the contributions to the total consumed current from each recombination channel. Remarkably, although the extracted parameters  $A' \sim D'$  depend on the numerical values of  $B$ ,  $V_{\text{active}}$ , and  $\text{IQE}_{\text{peak}}$ , the quality of fits as well as the individual contributions from each recombination channel ( $A'n$ ,  $B'n^2$ ,  $C'n^3$ , and  $D'n^4$  channels) is independent of these numerical values; instead, they are solely determined by the  $I$ -versus- $\sqrt{\text{IQE}_{\text{normalized}} \cdot I}$  dependence [see Eqs. (4) and (6)]. Because the  $I$ -versus- $\sqrt{\text{IQE}_{\text{normalized}} \cdot I}$  dependence is directly measured in experiments, no specific numerical values of  $B$  and  $V_{\text{active}}$  need to be assumed to obtain the results above. The absolute IQE values and the contribution of the  $Bn^2$  channel in Fig. 2 are determined by using  $\text{IQE}_{\text{peak,LED-1}} = 74\%$  and  $\text{IQE}_{\text{peak,LED-2}} = 40\%$ , which are derived as follows: the experimental  $I$ -versus- $\sqrt{\text{IQE}_{\text{normalized}} \cdot I}$  dependences allow us to determine  $B/B'_{\text{LED-1}} \times 74\% = \text{IQE}_{\text{peak,LED-1}}$  and  $B/B'_{\text{LED-2}} \times 90\% = \text{IQE}_{\text{peak,LED-2}}$  for LED-1 and LED-2, respectively. Since LED-1 has very high peak external quantum efficiency ( $\sim 50\%$ ), the second-order nonradiative term is assumed to be much smaller than the second-order radiative term,<sup>2</sup> that is  $B'_{\text{LED-1}} \approx B$ . This results in an  $\text{IQE}_{\text{peak}}$  of 74% for LED-1. We also assume that the two samples in Fig. 1(b) (both are wafer-based with the same chip area) have similar light-extraction efficiencies; therefore,  $\text{IQE}_{\text{peak,LED-2}} = 40\%$  can be estimated from the peak-efficiency ratio of the two samples, as shown in Fig. 1(b).

Since droop is a high-current phenomenon, we attribute the  $A'n$  term to the SRH recombination, or  $A' \approx A$ . For LED-1 with very high peak efficiency (74%),  $B'_{\text{LED-1}} \approx B$  has been assumed. At high currents, the fourth-order term is comparable to the third-order term, as shown in Fig. 2(c); for LED-2 with relatively low peak efficiency (40%), one finds  $B/B'_{\text{LED-2}} = 44.5\%$ , indicating a significant contribution of the nonradiative second-order term. The  $B/B'_{\text{LED-2}}$  ratio follows  $B/B'_{\text{LED-2}} \times 90\% = \text{IQE}_{\text{peak,LED-2}}$ , as shown above. One can conclude that for any reasonable  $\text{IQE}_{\text{peak}}$  value ( $< 90\%$ ) for LED-2, a nonradiative second-order contribution exists. A second-order nonradiative contribution has indeed been proposed by other authors.<sup>13</sup> At high currents, the contribution from the fourth-order term is stronger than that from the third-order term, as shown in Fig. 2(d). These results indicate that the droop-causing mechanism can have significant second, third, and fourth power contributions. The existence of strong second and fourth power contributions (stronger than the third power contribution) cannot be explained by the Auger recombination (with and without phase-space filling).

We notice that IQE-versus- $n$  curves at high currents can even be skewed to the right (see, for example, Fig. 2 of Ref. 11). The right-skewed IQE-versus- $n$  curve indicates the existence of negative high-order terms at high currents. It was calculated that based on the ABC model, an upper limit of Auger coefficient is  $1 \times 10^{-31} \text{ cm}^6 \text{ s}^{-1}$  (Ref. 14) for GaInN material to achieve lasing at a low experimental threshold current density of  $960 \text{ A/cm}^2$ .<sup>15</sup> While the third-order coefficient obtained from several experiments is larger than this value,<sup>2,5-8,13,16</sup> the lasing at low threshold current may be made possible by the existence of negative high-order terms

in  $R$ , which together with other high-order terms would invalidate the ABC model at high injections and, at high currents, reduce the droop-causing mechanisms thereby enabling lasing. This could be consistent with a carrier leakage mechanism: negative high-order terms could be caused by the screening of polarization field at high injection currents, therefore enabling carriers to be captured into QWs more efficiently instead of contributing to the carrier leakage.

In conclusion, we show that the ABC model used to describe carrier recombination in the active region of a LED necessarily results in IQE-versus- $n$  curves that have even symmetry. This finding holds even if phase-space filling is taken into account. In contrast, for a wide variety of samples, experimental IQE-versus- $n$  curves exhibit asymmetry. The asymmetry requires a fourth-power or higher-power contribution to the recombination rate and provides insight into the mathematical form of the droop-causing mechanisms.

Sandia authors and Q.D., Q.S., and J.C. were supported by Sandia's Solid-State Lighting Science Center, an Energy Frontier Research Center funded by the U.S. Department of Energy Office of Basic Energy Sciences. Sandia is a multi-program laboratory managed and operated by Sandia Corporation, a wholly owned subsidiary of Lockheed Martin Co., for the U.S. Department of Energy's National Nuclear Security Administration under Contract No. DE-AC04-94AL85000. The RPI authors gratefully thank Samsung LED, the National Science Foundation, New York State, Crystal IS, and Troy Research Corporation for support of E.F.S., M.H.K., Y.P., and RPI facilities.

<sup>1</sup>M.-H. Kim, M. F. Schubert, Q. Dai, J. K. Kim, E. F. Schubert, J. Piprek, and Y. Park, *Appl. Phys. Lett.* **91**, 183507 (2007).

<sup>2</sup>Q. Dai, Q. Shan, J. Wang, S. Chhajed, J. Cho, E. F. Schubert, M. H. Crawford, D. D. Koleske, M.-H. Kim, and Y. Park, *Appl. Phys. Lett.* **97**, 133507 (2010).

<sup>3</sup>J. Xie, X. Ni, Q. Fan, R. Shimada, Ü. Özgür, and H. Morkoç, *Appl. Phys. Lett.* **93**, 121107 (2008).

<sup>4</sup>A. Y. Kim, W. Götz, D. A. Steigerwald, J. J. Wierer, N. F. Gardner, J. Sun, S. A. Stockman, P. S. Martin, M. R. Krames, R. S. Kern, and F. M. Steranka, *Phys. Status Solidi A* **188**, 15 (2001).

<sup>5</sup>Y. C. Shen, G. O. Mueller, S. Watanabe, N. F. Gardner, A. Munkholm, and M. R. Krames, *Appl. Phys. Lett.* **91**, 141101 (2007).

<sup>6</sup>M. Zhang, P. Bhattacharya, J. Singh, and J. Hinckley, *Appl. Phys. Lett.* **95**, 201108 (2009).

<sup>7</sup>A. David and M. J. Grundmann, *Appl. Phys. Lett.* **96**, 103504 (2010).

<sup>8</sup>J. Hader, J. V. Moloney, B. Pasenow, S. W. Koch, M. Sabathil, N. Linder, and S. Lutgen, *Appl. Phys. Lett.* **92**, 261103 (2008).

<sup>9</sup>K. J. Vampola, M. Iza, S. Keller, S. P. DenBaars, and S. Nakamura, *Appl. Phys. Lett.* **94**, 061116 (2009).

<sup>10</sup>Q. Shan, Q. Dai, S. Chhajed, J. Cho, and E. F. Schubert, *J. Appl. Phys.* **108**, 084504 (2010).

<sup>11</sup>A. David and M. J. Grundmann, *Appl. Phys. Lett.* **97**, 033501 (2010).

<sup>12</sup>N. F. Gardner, G. O. Mueller, Y. C. Shen, G. Chen, S. Watanabe, W. Götz, and M. R. Krames, *Appl. Phys. Lett.* **91**, 243506 (2007).

<sup>13</sup>J. Hader, J. V. Moloney, and S. W. Koch, *Appl. Phys. Lett.* **96**, 221106 (2010).

<sup>14</sup>A. Hangleiter, International Conference on Nitride Semiconductors (ICNS), Jeju, Korea, 18–23 October 2009.

<sup>15</sup>H. Y. Ryu, K. H. Ha, J. K. Son, S. N. Lee, H. S. Paek, T. Jang, Y. J. Sung, K. S. Kim, H. K. Kim, Y. Park, and O. H. Nam, *Appl. Phys. Lett.* **93**, 011105 (2008).

<sup>16</sup>H.-Y. Ryu, H.-S. Kim, and J.-I. Shim, *Appl. Phys. Lett.* **95**, 081114 (2009).